

RECENT DEVELOPMENTS IN WELL TEST ANALYSIS
IN THE STANFORD GEOTHERMAL PROGRAM

C. Ehlig-Economides
Department of Petroleum Engineering
Stanford University
Stanford, California 94305

In the past year a number of studies pertaining to geothermal well test analysis were conducted. In this paper a brief overview of progress on the following six subjects is presented: (1) earth tide effects on a closed reservoir, (2) transient pressure analysis of multilayered heterogeneous reservoirs, (3) interference testing with wellbore storage and skin at the producing well, (4) steam/water relative permeabilities, (5) transient rate and pressure buildup resulting from constant pressure production, and (6) transient pressure analysis of a parallelepiped reservoir.

Earth Tide Effects

The gravitational attraction between the sun, moon, and earth induces a radial deformation of the earth which results in the readily observable oceanic tides. The same mechanism also generates a state of stress on the surface of the earth which has been referred to as earth tides. Due to the low compressibility of the earth compared to that of water, the pressure transients caused by earth tides are of small amplitude. However, the pressure changes are of sufficient magnitude to cause water level variations in open wells and pits, and several investigators have indicated that a relationship exists between the amplitude of the response of an open well system and the characteristics of the formation and the fluid contained therein.

P. Arditty^{1,2} modified the equations solved by Bodvarsson³ for an open well in a finite closed reservoir to apply to a shut-in well with the borehole completely filled with formation fluid. Only one phase is flowing in the reservoir, and the reservoir is confined and infinite in radial extent. The expression for pressure induced by an applied tectonic pressure, p_a , is given by:

$$p = p_{SD} \left(1 - \frac{ae^{n(a-r)}}{r \left[1 + \frac{B}{i\omega} \left(\frac{1}{a} + n \right) \right]} \right) \quad (1)$$

with:

$$p_a = p_{SD} \left(1 - \frac{1}{1 + \frac{B}{i\omega a} (na+1)} \right) \quad (2)$$

where $B = 4k/c_f \mu \ell$, $n^2 = i\omega/d$, ω = oscillation frequency, d = diffusivity $k/\mu c_f$, ℓ = wellbore radius, and r = radial distance from well. The static pressure $p_a = p_{SD} (4G_c - c_m)/(3+4G_c)$, where p_{SD} is an applied tectonic pressure, G_c is the rock matrix shear modulus, c_f is fluid compressibility, and c_m is matrix compressibility. The amplitude of the relative response p_a/p_{SD} is:

$$R_e(p_a/p_{SD}) \approx R_e \left(\frac{\frac{4k/i\omega\mu\ell c_f}{4k}}{1 + \frac{4k}{i\omega\mu\ell c_f}} \right) \quad (3)$$

The critical frequency, ω_c for which the response amplitude exhibits an abrupt decrease is defined by:

$$\omega_c = \frac{4k}{\mu\ell c_f} \quad (4)$$

Tides are classified according to length of period, T : long period tides ($T = 16$ days); diurnal tides ($T = 1$ day), semidiurnal tides ($T = 1/2$ day); and terdiurnal tides ($T = 1/3$ day). If $\omega_c/2\pi \gg 2$, then the critical frequency exceeds both the diurnal and semidiurnal frequencies, and $A_D/A_{SD} = 1$, where A_D and A_{SD} are the diurnal and semidiurnal amplitudes of the earth tide effect. If $1 < \omega_c/2\pi < 2$, then $1.25 < A_D/A_{SD} < 2$. If $\omega_c/2\pi \ll 1$, both amplitudes will be small, and undetectable. Thus, the ratio of the two amplitudes determines limits on the value of ω_c , which in turn gives an approximation for $k/\mu c_f$ since ℓ and ω_c are known. If ω_c is computed from $k/\mu c_f$, an explanation for existence or nonexistence of tidal effects is provided.

A graph of amplitude versus period for a typical sandstone reservoir containing gas is shown in Fig. 1. From these results we would expect the diurnal tide amplitude to exceed the semidiurnal tide amplitude and both should be detectable.

Figure 3 shows raw data from a fluid test. Figure 4 shows the data in Fig. 3 modified to show relative pressure variations. Spectral analysis using Fast Fourier Transforms provides the results shown in Fig. 5. The two small peaks in amplitude are due to diurnal and semidiurnal tide effects. The reader is referred to Ref. 1 and Ref. 2 for more detail..

Multilayered Systems

A mathematical model was derived by S. Tariq^{4,5} to satisfy the following conditions for a multilayered reservoir: each layer is horizontal and circular, homogeneous and isotropic, and bounded by impermeable formations at the top, bottom, and at the external drainage radius. Each layer has constant porosity and permeability, and

uniform thickness, but the drainage radius may be different for different layers. The fluid in each layer has **small** and constant compressibility. Initial reservoir pressure is the same for each layer; and instantaneous sandface pressure is identical for all layers. Pressure gradients are small and gravity effects negligible. The total production rate, q , is constant, but the production rate for each layer may vary in time. The model for n layers is specified by the following equations:

$$\frac{\partial^2 p_j}{\partial r^2} + \frac{1}{r} \frac{\partial p_j}{\partial r} = \frac{\phi_j \mu_j C_j}{k_j} \frac{\partial p_j}{\partial t} ; p_j(r, t) = p_i - p_j(r, t), r \in [r_{wj}, r_{ej}] \quad (5)$$

$$p_j(r, 0) = 0 \quad (6)$$

$$\frac{\partial p_j}{\partial r}(r_{ej}, t) = 0 \quad (7)$$

$$p_{wf}(t) = p_j(r_w, t) - s_j \left(r \frac{\partial p_j}{\partial r} \right)_{r_w} \quad (8)$$

$$\begin{aligned} q &= C \frac{\partial p_{wf}}{\partial t} + \sum_{j=1}^n q_j(t) \\ &= C \frac{dp_{wf}}{dt} - 2\pi \sum_{j=1}^n \left(\frac{kh}{\mu} \right)_j \left(r \frac{\partial p_j}{\partial r} \right)_{r_{wj}} \end{aligned} \quad (9)$$

where $j = 1, 2, \dots, n$; s_j = skin factor for each layer; and C = wellbore storage constant cc/atm .

The system of equations is transformed into and solved in Laplace space. The resulting solution is then numerically inverted using the algorithm by Stehfest.

A thorough analysis of drawdown data generated for different types of layered **systems** was conducted. The cases investigated included **layers** having different permeabilities, thicknesses, radii, and **skin** effects. Log-log type curves for analysis of multilayered systems were developed, and techniques for analyzing two-layered systems using semilog graphs of pressure vs time were described. The reader is referred to Ref. 4 and Ref. 5 for more detail.

Interference Testing

As more sensitive pressure gauges have become available, interference testing, that is, observation of the pressure changes at a shut-in well resulting from a nearby producing well, has become feasible. Interference testing has the advantage of investigating more reservoir volume than a single-well test. For a producing well with considerable wellbore storage and skin effects, the combined effects of the storage and skin is to prolong the time it takes for the sandface flow rate to become equal to the surface flow rate. Since the sandface flow rate is not constant during this time period, conventional interference testing, which assumes a constant rate, is not valid.

The mathematical model used in this study by H. Sandal^{7,8} assumes the flow is radial, the medium is infinite, homogeneous, and isotropic with constant porosity and permeability, the single-phase fluid is slightly compressible with constant viscosity, pressure gradients are small, and wellbore storage and skin are constant. The equations which represent this system are the following:

$$\frac{\partial^2 p_D}{\partial r_D^2} + \frac{1}{r_D} \frac{\partial p_D}{\partial r_D} = \frac{\partial p_D}{\partial t_D} ; \quad p_D = p_D(r_D, t_D), \quad r_D > 1, \quad t_D > 0 \quad (10)$$

$$p_D(r_D, 0) = 0 ; \quad r_D > 1 \quad (11)$$

$$c_D \frac{\partial p_{wD}}{\partial t_D} - \left. \frac{\partial p_D}{\partial r_D} \right|_{r_D=1} = 1 ; \quad t_D > 0 \quad (12)$$

$$p_{wD} = p_D - \left. S \frac{\partial p_D}{\partial r_D} \right|_{r_D=1} ; \quad t_D > 0 \quad (13)$$

$$\lim_{r_D \rightarrow \infty} p_D(r_D, t_D) = 0 ; \quad t_D > 0 \quad (14)$$

where p_D , r_D , t_D , and c_D are dimensionless pressure drop, radius, time, and storage, respectively, p_{wD} is the pressure drop inside the wellbore, and S is the wellbore skin factor.

The equations are transformed into and solved in Laplace space. The resulting Laplace space solution is numerically inverted using the Stehfest⁶ algorithm.

Results were compared with the study by Garcia-Rivera and Raghavan which was based on the superposition of a series of line source solutions combined with sandface flow rates obtained for a finite radius well (Ramey and Agarwal, and Ramey, Agarwal, and Martin¹¹). The comparison indicated that for low values of the effective wellbore radius, $C_D e^{\frac{1}{2}s}$, the Garcia-Rivera and Raghavan study may be in error. Figure 5 shows the close agreement between the two solutions for large values of $C_D e^{\frac{1}{2}s}$. Figure 6 shows an example of discrepancies between the two solutions. The reader is referred to Ref. 7 and Ref. 8 for more detail.

Steam/Water Relative Permeabilities

Using production data from the Wairakei field, R. Horne¹² and K. Shinohara¹³ demonstrated that steam/water relative permeability curves can be generated from field data. The method of analysis was suggested by Grant,¹⁴ but improvements were made on the production data. Specifically, assuming negligible wellbore heat loss, steam and water discharges at the wellbase were back calculated from the surface values. The wellbore heat loss was less than 1% in the wells tested because they have been flowing for a long period of time. Total discharge values were divided by the wellhead pressure in order to filter out changes in discharge due only to pressure depletion in the reservoir. Thus, changes in discharge due to relative permeability effects were isolated. The actual downhole temperature was used to determine fluid densities, viscosities, and enthalpies. Finally, flowing water saturation was determined from the back-calculated wellbase steam and water discharges. They did not take into account the immobile fluid in the reservoir.

Relative permeabilities were computed from equations for Darcy's law and the flowing enthalpy given below:

$$q_w = - \rho_w \frac{k}{\mu_w} F_w(S_w) A p' \quad (15)$$

$$q_s = - \rho_s \frac{k}{\mu_s} F_s(S_w) A p' \quad (16)$$

$$h = \frac{\rho_w h F_w(S_w)/\mu_w + \rho_s h F_s(S_w)/\mu_s}{\rho_w F_w(S_w)/\mu_w + \rho_s F_s(S_w)/\mu_s} \quad (17)$$

where q is the discharge rate, ρ is one-phase fluid density, μ is viscosity, A is flow area, p is the pressure gradient, F is the fractional flow, S_w is the flowing water saturation, and subscripts

s and **w** refer to the steam and water phases. Figure 7 shows the resulting permeability curves.

Future improvements on this method will include incorporation of wellbore heat loss in the back calculation of fractional flow, and use of irreducible water saturations estimated from results of experimental studies in the Stanford Geothermal Program.

Constant Pressure Production

Conventional well test analysis has been developed primarily for constant rate production. Since there are a number of common reservoir production conditions which result in constant pressure production, there is a need for a more thorough treatment of transient rate analysis and pressure buildup after constant pressure production.

In this work by C. Ehlig-Economides, the following assumptions are needed: flow is strictly radial, and the porous medium is homogeneous and isotropic, with constant thickness h , porosity ϕ , and permeability k . The fluid viscosity is constant, and the total compressibility of the fluid and the porous medium is small in magnitude and constant. The equations to be solved are the following:

$$\frac{\partial^2 p_D}{\partial r_D^2} + \frac{1}{r_D} \frac{\partial p_D}{\partial r_D} = \frac{\partial p_D}{\partial t_D} ; \quad p_D = p_D(r_D, t_D), \quad r_D \in [1, R], \quad t_D > 0 \quad (18)$$

$$p_D(r_D, 0) = 0 ; \quad r_D \in [1, R] \quad (19)$$

$$p_D(1, t) = 1 + S \lim_{r_D \rightarrow 1^+} \frac{\partial p_D}{\partial r_D} ; \quad (t_D > 0) \quad (20)$$

$$\lim_{r_D \rightarrow \infty} p_D(r_D, t_D) = 0 ; \quad (t_D > 0) \quad \text{for unbounded reservoir} \quad (21)$$

$$\frac{\partial p_D}{\partial r_D}(R, t_D) = 0 ; \quad (t_D > 0) \quad \text{for closed bounded reservoirs, } R = \frac{r_e}{r_w} \quad (22)$$

$$p_D(R, t_D) = 0 ; \quad (t_D > 0) \quad \text{for constant pressure bounded reservoir} \quad (23)$$

$$q_D(t_D) = - \lim_{r_D \rightarrow 1^+} \frac{\partial p_D}{\partial r_D} \quad (24)$$

where:

$$r_D = r/r_w, \quad t_D = \frac{kt}{\phi \mu c r_w^2}, \quad p_D(r_D, t_D) = \frac{p_i - p(r_D, t_D)}{p_i - p_w},$$

$$q_D = \frac{q\mu}{2\pi kh(p_i - p_w)}, \quad \text{and } S \text{ is wellbore skin factor.}$$

Transient rate solutions have been tabulated in the literature. In this work, the numerical Laplace inverter by Stehfest⁶ is used to generate solutions for the transient wellbore rate, the radial pressure distribution, and cumulative production including boundary and skin effects.

Pressure buildup after constant pressure production has not been properly handled in the literature. It can be shown that the following equation exactly represents pressure buildup after constant production under the conditions mentioned at the beginning of this section.

$$p_{DS}(\Delta t_D) = 1 + \int_{t_{Df}}^{t_{Df} + \Delta t_D} q_D(\tau) \frac{dp_{Dw}}{d\tau} (t_{Df} + \Delta t_D - \tau) d\tau \quad (25)$$

where p_{DS} is the dimensionless shut-in pressure at the wellbore, t_{Df} is the flowing time before shut-in, Δt_D is the elapsed time after shut-in, q_D is dimensionless rate, defined above, and p_{Dw} is the dimensionless wellbore pressure drop for constant rate production, defined by:

$$p_{Dw}(t_D) = \frac{2\pi kh}{q\mu} (p_i - p[1, t_D]).$$

This work is nearing completion. The author may be consulted for more information.

Parallelepiped Model

The parallelepiped model has been proposed as a reasonable approximation for both The Geysers and the Italian geothermal reservoirs. Through use of source functions, Green's functions, and the Neumann product method described by Gringarten, 15 solutions are readily available for a number of related problems. The model assumes three-dimensional flow in a reservoir bounded by impermeable and/or constant pressure boundaries with a well located at any point which may be

fully or partially penetrated and which may intersect a horizontal or a vertical fracture. Solutions are in the form of infinite sums and integrals which must be integrated by computer. Type-curves are being developed which will shed new light on the behavior of geothermal reservoirs. In particular, detection of a boiling front may be possible in a dry steam reservoir bounded at its base by boiling water. This constitutes a constant pressure boundary if the reservoir is isothermal.

References

1. Arditty, P.C., and Ramey, H.J., Jr.: "Response of a Closed Well-Reservoir System to Stress Induced by Earth Tides," Paper SPE 7484, presented at the 53rd Annual Fall Meeting of the SPE of AIME, Oct. 1978, Houston, Texas.
2. Arditty, P.C.: "The Earth Tide Effects on Petroleum Reservoirs, Preliminary Study," Engineer's Degree Thesis, Stanford University Petroleum Engineering Department, 1978.
3. Bodvarsson, G.: "Confined Fluid as Strain Meters," J. Geoph. Res. (1970), 75, No. 14, p. 2711.
4. Tariq, S.M., and Ramey, H.J., Jr.: "Drawdown Behavior of a Well with Storage and Skin Effect Communicating with Layers of Different Radii and Other Characteristics," Paper SPE 7453, presented at the 53rd Annual Fall Meeting of the SPE of AIME, Oct. 1978, Houston, Texas.
5. Tariq, S.M.: "A Study of the Behavior of Layered Reservoirs with Wellbore Storage and Skin Effect," Ph.D. Dissertation, Stanford University Petroleum Engineering Department, 1977.
6. Stehfest, H.: "Numerical Inversion of Laplace Transforms," Communications of the ACM (Jan. 1970), 13, No. 1, Algorithm 368.
7. Sandal, H.J., Horne, R.N., Ramey, H.J., Jr., and Williamson, J.W.: "Interference Testing with Wellbore Storage and Skin Effect at the Produced Well," Paper SPE 7454, presented at the 53rd Annual Fall Meeting of the SPE of AIME, Oct. 1978, Houston, Texas.
8. Sandal, H.J. : "Interference Testing with Skin and Storage," Engineer's Degree Thesis, Stanford University Petroleum Engineering Department, 1978.
9. Garcia-Rivera, J., and Raghavan, R. : "Analysis of Short-Time Pressure Transient Data Dominated by Wellbore Storage and Skin at Unfractured Active and Observation Wells," Paper SPE 6546, presented at the 47th Annual California Regional Meeting of the SPE of AIME, Apr. 1977, Bakersfield, CA.
10. Ramey, H.J., Jr., and Agarwal, R.G. : "Annulus Unloading Rates and Wellbore Storage," Soc. Pet. Eng. J. (Oct. 1972), 453-462.

11. Ramey, H.J., Jr., Agarwal, R.G., and Martin, I.: "Analysis of 'Slug Test' or DST Flow Period Data," J. Can. Pet. Tech. (July-Sept. 1975), 34-47.
12. Horne, RN, and Ramey, H.J., Jr.: "Steam/Water Relative Permeabilities from Production Data," Geothermal Resources Council, Trans. (July 1978), 2.
13. Shinohara, K. : "Calculation and Use of Steam/Water Relative Permeabilities in Geothermal Reservoirs," M.S. Report, Stanford University Petroleum Engineering Department, 1978,
14. Grant, M.A.: "Permeability Reduction Factors at Wairakei," presented at the AIChE-ASME Heat Transfer conference, Salt Lake City, Utah, Aug. 15-17, 1977.
15. Gringarten, AC, and Ramey, H.J., Jr.: "The Use of Source and Green's Functions in the Solution of Unsteady Flow Problems in Reservoirs," Soc. Pet. Eng. J. (Oct. 1973), 285-296; Trans. AIME, 255.

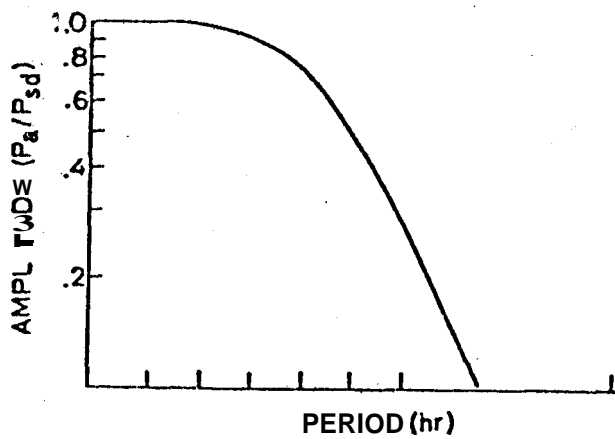


FIG. 1: RESPONSE (P_a/P_{sd}) OF A CLOSED-WELL RESERVOIR SYSTEM FOR A SANDSTONE CONTAINING GAS

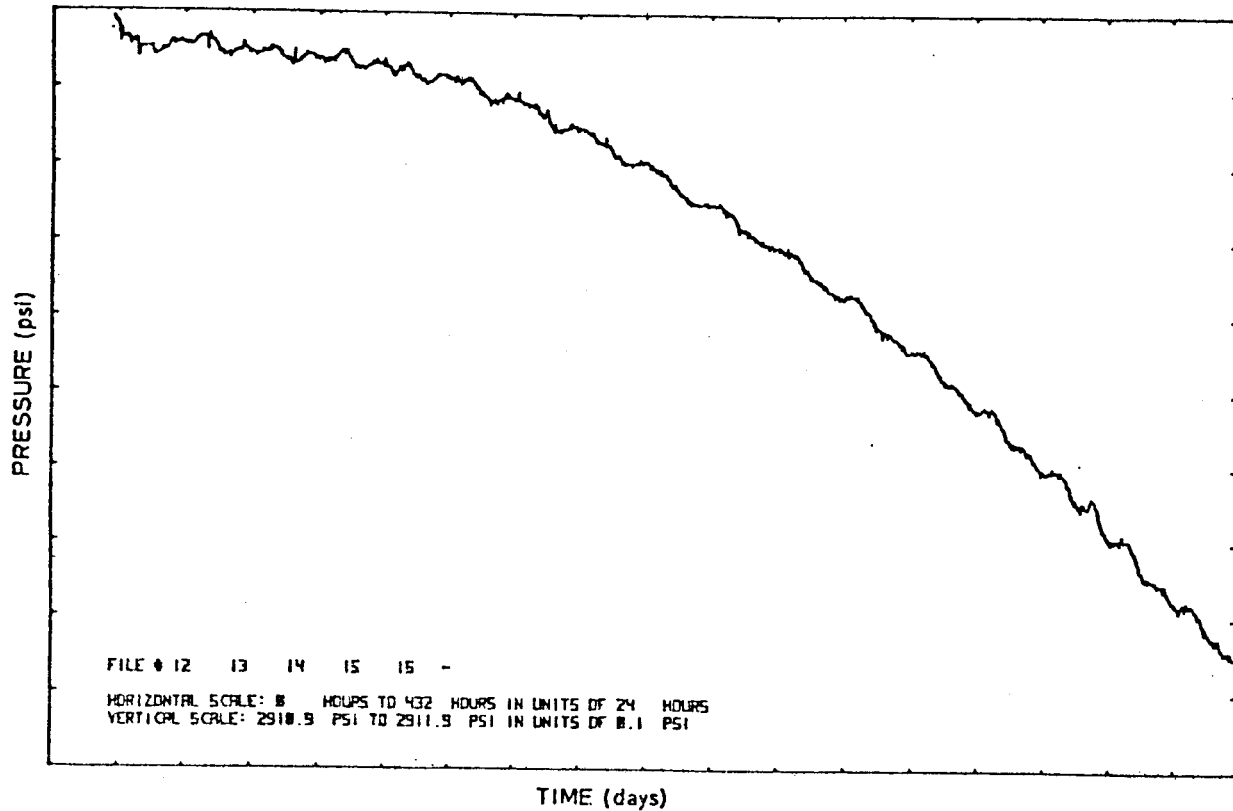


FIG. 2 : INITIAL DATA FOR THE "A" FIELD

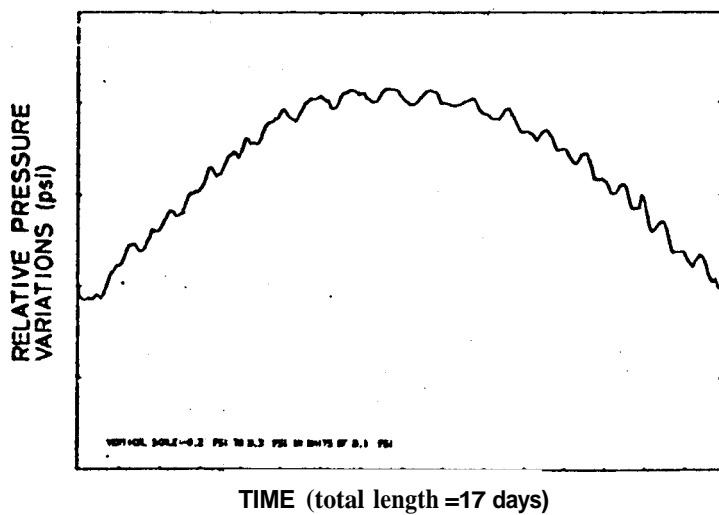


FIG. 3: MODIFIED DATA FOR THE "A" FIELD

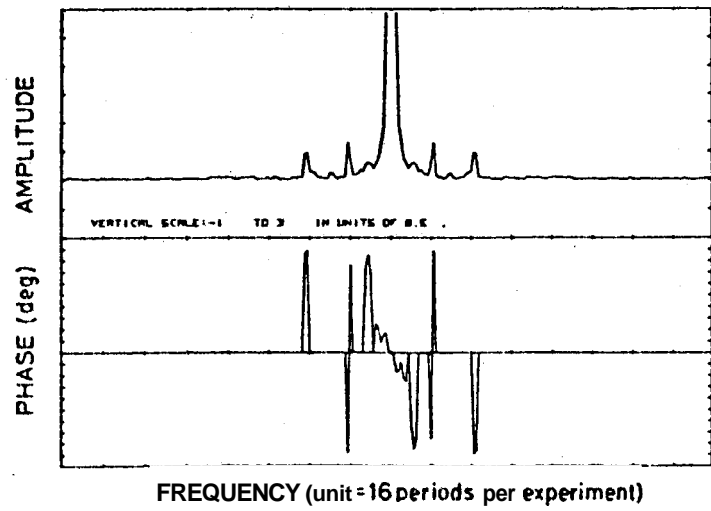


FIG. 4; SPECTRUM ANALYSIS BY FFT FOR "A" FIELD

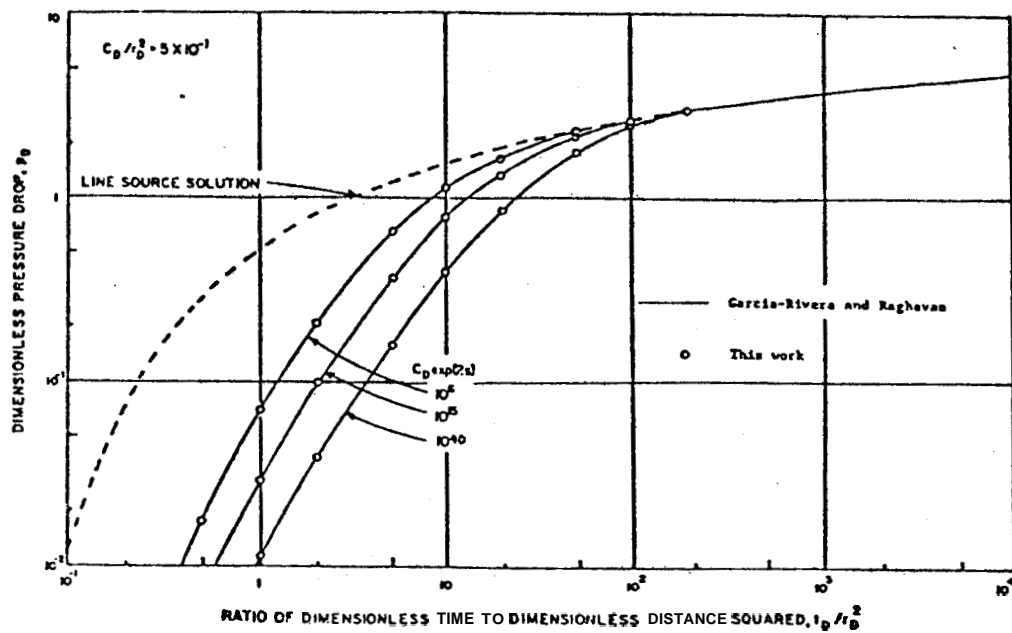


FIG. 5: COMPARISON OF RESULTS OF THIS STUDY WITH THE GARCIA-RIVERA AND RAGHAVAN STUDY

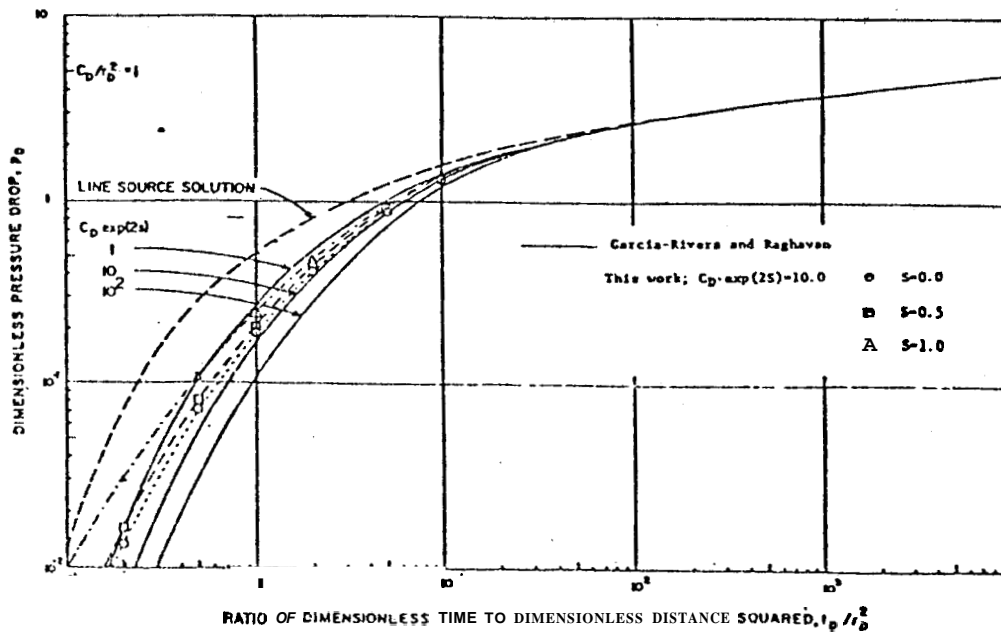


FIG. 6: COMPARISON OF RESULTS OF THIS STUDY WITH THE GARCIA-RIVERA AND RAGHAVAN STUDY

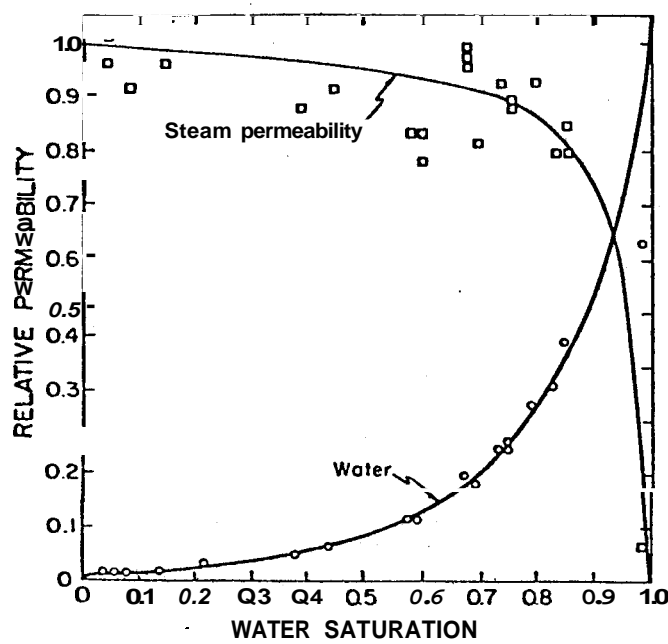


FIG. 7: STEAM-WATER RELATIVE PERMEABILITIES FROM WAIRAKEI WELL DATA